Cellulose (2012) 19:751–760
DOI 10.1007/s10570-012-9688-2

ORIGINAL PAPER

Compression molded wood pulp biocomposites: a study of hemicellulose influence on cellulose supramolecular structure and material properties

Helena Nilsson · Sylvain Galland · Per Tomas Larsson · E. Kristofer Gamstedt · Tommy Iversen

Received: 12 October 2011 / Accepted: 6 March 2012 / Published online: 23 March 2012

Abstract In this study, the importance of hemicellulose content and structure in chemical pulps on the property relationships in compression molded wood pulp biocomposites is examined. Three different softwood pulps are compared; an acid sulfite dissolving grade pulp with high cellulose purity, an acid sulfite paper grade pulp and a paper grade kraft pulp, the latter two both containing higher amounts of hemicelluloses. Biocomposites based the acid sulfite pulps exhibit twice as high Young's modulus as the composite based on paper grade kraft pulp, 11–12 and 6 GPa, respectively, and the explanation is most likely the difference in beating response of the pulps. Also the water retention value (WRV) is similarly low for the two molded sulfite pulps (0.5 g/g) as compared to the molded kraft pulp (0.9 g/g). The carbohydrate composition is determined by neutral sugar analysis and average molar masses by SEC. The cellulose supramolecular structure (cellulose fibril aggregation) is studied by solid state CP/MAS ^{13}C-NMR and two forms of hemicellulose are assigned. During compression molding, cellulose fibril aggregation occurs to higher extent in the acid sulfite pulps as compared to the kraft pulp. In conclusion, the most important observation from this study is that the difference in hemicellulose content and structure seems to affect the aggregation behaviour and WRV of the investigated biocomposites.

Keywords CP/MAS ^{13}C-NMR · Compression molding · Chemical pulps · Mechanical properties · Hemicelluloses · Fibril aggregation · Composites

Introduction

The native wood fiber cell wall is a hierarchical structure consisting of aggregated cellulose fibrils embedded in a matrix of mainly hemicellulose and lignin. The elementary cellulose fibrils with a lateral dimension of around 3.5 nm (Fengel and Wegner 1984) consists of linear and long cellulose chains with numerous polar groups, arranged into an extensive hydrogen bond network, giving the fibril a crystalline core and a less-ordered fibril surface (para-crystalline

H. Nilsson · S. Galland · P. T. Larsson · T. Iversen
Wallenberg Wood Science Center, Royal Institute of Technology, 100 44 Stockholm, Sweden

H. Nilsson (✉) · P. T. Larsson · T. Iversen (✉)
Innventia AB, P.O. Box 5604, 114 86 Stockholm, Sweden
e-mail: helena.nilsson@innventia.com

T. Iversen
e-mail: tommy.iversen@innventia.com

E. K. Gamstedt
Department of Engineering Sciences, Uppsala University, P.O. Box 534, 751 21 Uppsala, Sweden

cellulose) (Frey-Wyssling 1954). These fibrils are aggregated into larger structures, aggregated cellulose fibrils (microfibrils), with a lateral dimension of 10–30 nm (Fengel and Wegner 1984; Hult et al. 2000). Due to the nanometric lateral dimensions, micrometric lengths and oriented semi-crystalline structure of the cellulose fibril aggregates they possess excellent mechanical properties in the axial fibril direction (Nishino et al. 1995). The Young's modulus of the cellulose fibril exceeds 100 GPa (Sakurada et al. 1962; Nishino et al. 1995; Iwamoto et al. 2009) and cellulose based biocomposites could therefore be a potential replacement of inorganic fibers such as carbon or glass, resulting in a renewable nanocomposite with lower raw material cost.

In a previous study (Nilsson et al. 2010) it was shown that high stiffness all-cellulose I composite materials composed of commercial dissolving pulps with high cellulose purity could be produced by compression molding at elevated temperatures with water as the only processing aid. In the present study the importance of hemicellulose content and structure in chemical pulps on the water-holding and mechanical property relationships in compression molded hemicellulose containing wood pulp biocomposites are examined. Three different softwood pulps are compared; an acid sulfite dissolving grade pulp with high cellulose purity, an acid sulfite paper grade pulp and a paper grade kraft pulp, the latter two both containing higher amounts of hemicelluloses.

The objective of this study is to examine effects of pulping process and hemicelluloses composition/structure on cell wall nanostructure in the compression molded materials. Due to the complex supramolecular structure of cellulose several models and methods to describe the structure can be found and is constantly added in the literature. In a series of papers (Larsson et al. 1997; Wickholm et al. 1998; Hult et al. 2000) it has been shown that cross polarization/magic angle spinning carbon 13 nuclear magnetic resonance (CP/MAS ^{13}C-NMR) spectroscopy is a powerful tool for investigation of cellulose I structure. If it is used in connection with spectral fitting of the C4 region the states of orders can be quantified and the cellulose fibril and fibril aggregate size can be determined. Therefore, in this study, the cell wall nanostructure of the biocomposites is examined by CP/MAS ^{13}C-NMR spectroscopy. In addition, mechanical properties are studied and discussed.

Experimental section

Materials

The totally chlorine free (TCF) bleached softwood acid sulfite pulps (80 % pine, 20 % spruce); a never-dried dissolving and a dried paper grade, were from Domsjö Fabriker AB, Sweden. The kraft pulp was a commercial never-dried TCF-bleached Scandinavian softwood kraft pulp.

Processing of all-cellulose biocomposites

Wet pulp (dry weight 30 g) was disintegrated (ISO 5263-1:2004), subjected to 30,000 revolutions in a standard disintegrator (Noram model G3-13, Lorentz and Wettre, Canada Inc.). Deionized water was added and the pulp was beaten in a PFI mill (ISO 5264-2:2002) at 4,000 revolutions, force per unit bar length 3.33 N/mm. After beating, laboratory hand-sheets were prepared (ISO 5269-1:2005). Dimensions of in-plane isotropic fiber sheets were 165 mm × 165 mm. Directly after forming, the sheets were cold-pressed in a PTI 40140 sheet press for 7 min under 0.6 MPa pressure to attain approximately 50 % dry mass content. Quarter parts of the handsheets were compression molded between blotters in a PHI press model 0230H at various temperatures, to obtain a plate of 80 × 80 mm. The pulp sheet and blotters were placed in the press pre-heated to 170 °C. Contact was kept between the blotters and the hot metallic plates for 5 min without pressure, followed by a rapid pressure increase to 45 MPa, maintained for 20 min. A 15 kg weight (resulting in a pressure of 23 kPa) was applied on the biocomposite plate to limit warping during cooling.

Neutral sugar analysis

Carbohydrate composition was determined after hydrolysis at 1.2 bar 120 °C with 0.4 M sulphuric acid, according to TAPPI T249 cm-00. The solubilized monosaccharides were quantified by high-performance anion exchange chromatography (HPAEC) with a Dionex DX 500 chromatography system coupled with pulsed amperometric detection (PAD, Dionex ED 40) and using a CarboPac PA-1 column (all from Dionex, Sunnyvale, CA, USA).

Size exclusion chromatography (SEC)

Samples (pre-swollen in deionized water for 7 days at room temperature) were solvent exchanged 3 times with lithium chloride/*N*,*N*-dimethylacetamide (LiCl/DMAc) and vibratory milled. The solvent was LiCl/DMAc and the chromatographic system consisted of four columns (Mixed-A 20 µm, 7.5 × 50 mm, Polymer Laboratories) in series with an Optilab DSP refractive index detector. The mobile phase was 0.5 % (w/v) LiCl/DMAc, at 0.36 ml/min, and the injection volume was 10 µl. Narrow pullulan standards were used for calibration and Waters Millennium software for data evaluation (Berthold et al. 2004). The two peaks being observed by the detector represents the hemicellulose fraction (low molecular mass) and the cellulose fraction (high molecular mass).

CP/MAS ^{13}C-NMR spectroscopy and spectral fitting

The samples (pre-swollen in deionized water 7 days at room temperature) were carefully disintegrated and packed in a zirconium oxide rotor. Sulfite paper grade and kraft pulp samples were hydrolyzed for 17 h in 2.5 M HCl (aq) at 100 °C in order to remove interfering signals from hemicelluloses (Hult et al. 2000). The sulfite dissolving grade pulp was not subjected to hydrolysis due to its already low content of hemicelluloses. CP/MAS ^{13}C-NMR spectra were recorded at 290 ± 1 K using a Bruker Avance AQS 300 WB instrument at 7.04 T. The MAS rate was 5 kHz. A 7 mm double air-bearing probe was used. Acquisition was performed with a CP pulse sequence, using a 4.3 µs proton 90° pulse, an 800 µs ramped (100–50 %) falling contact pulse and a 2.5 s delay between repetitions. A two-pulse phase modulation (TPPM15) pulse sequence was used for ^{1}H decoupling. Glycine was used for the Hartmann-Hahn matching procedure, as well as an external standard. The software developed at Innventia AB for spectral fitting of the C4-region based on a Levenberg–Marquardt algorithm was applied (Larsson et al. 1997; Wickholm et al. 1998). Five distinct lines were used for the spectral fitting; one Lorentzian line for the cellulose I ($\alpha + \beta$) allomorphs at 88.7 ppm, and four Gaussian lines for the non-crystalline cellulose forms: para-crystalline at 88.4 ppm, fibril surfaces being accessible to water at 84.2 and 83.2 ppm and fibril surfaces being inaccessible to water at 83.8 ppm (Larsson et al. 1997; Wickholm et al. 1998). By assuming a square cross section of fibrils and cellulose fibrils aggregates, and a glucan chain width of 0.57 nm, lateral dimensions for fibrils and cellulose fibril aggregates were estimated from integrated signal intensities for the C4 region and the C4 surface signals (Larsson et al. 1997; Wickholm et al. 1998; Teleman et al 2001; Zhou et al. 2009; Malm et al. 2009). For the non-hydrolyzed paper grade pulps an additional line at 81.0 ppm representing the hemicelluloses localized at fiber surfaces was added (Wickholm et al. 1998; Hult et al. 2000; Teleman et al 2001). For these samples the line at 83.5 ppm included not only fibril surfaces being inaccessible to water but also inaccessible hemicelluloses, which could be estimated by subtracting the intensity of the hemicellulose signal at 81.0 ppm from the total hemicellulose content in mol% based on neutral sugar analysis calculations according to Jansson (1970).

Modified water retention value (WRV)

A modified method of SCAN-C 62:00 was used to measure the WRV of the compression molded samples according to Nilsson et al. (2010). The samples were pre-swollen in deionized water 10–12 days at room temperature prior centrifugation of 40–50 mg at 3,000×*g* for 15 min in a centrifuge tube filter (VectraSpin$^{\mathrm{TM}}$ 3, 10 µm polypropylene mesh 3 ml, Whatman International Ltd.). After centrifugation, samples were transferred into weighing bottles and weighed before and after drying in oven overnight at 105 °C. The WRV is a measure of water-holding capacity and was calculated as the ratio between the mass of water retained in the fibers after centrifugation and the dry mass. Two WRV measurements were made for each sample.

Mechanical characterization

Dog bone shaped samples (ISO 37-3, 4 mm wide, 0.9 mm thick) were laser cut from conditioned cellulose plates. The samples were conditioned (48 h) and tensile tested at 23 °C and 50 % RH on an Instron 5566 equipped with a video extensometer and a 500 N load cell. Ultimate strength, Young's modulus and strain to failure were measured. Crosshead speed was 10 mm/min. A minimum of 8 specimens were tested per sample. Density at 50 % RH was obtained by relating mass to volume calculated from thickness and surface area of samples.

Field emission microscopy (FE-SEM)

Cross-sections of samples fractured during tensile testing were observed in a Philips 30XL ESEM-FEG (environmental scanning electron microscope–field emission gun), with prior sputtering of 5 nm thick gold–palladium coating using a Baltec SCD 005 sputter coater.

Results and discussion

Carbohydrate composition and cellulose supramolecular structure

The selected chemical pulps were chosen for their large variation in process history while having similar initial cellulose fibril aggregate widths. The carbohydrate composition and molecular masses of the polysaccharides in the different pulps are presented in Table 1. It is well known that chemical pulps from softwood contain both galactoglucomannan and arabinoglucuronoxylan, the former dominating in sulfite pulps and the latter in kraft pulps (Petterson and Rydholm 1960), which is confirmed by the neutral sugar analyses. As mentioned in the introduction, the glucose content is higher in the sulfite dissolving grade pulp (95.8 wt%) than in both the sulfite paper grade (88.8 wt%) and the kraft pulp (84.9 wt%). Regarding the average molar masses in Table 1 it is shown that the cellulose molar mass approximated by the high molar mass fraction in kraft and sulfite paper grade pulp is significantly higher than in the sulfite dissolving grade pulp, this due to acid hydrolysis during the harsher cooking stage for the dissolving pulp. On the other hand, the average molar mass of the low molar mass fraction assigned mainly to the hemicelluloses for the kraft pulp is much higher than for both of the two sulfite pulps.

By spectral fitting of the C4 region of the CP/MAS ^{13}C-NMR spectrum it is possible extract information about the cellulose supramolecular structure, especially on pure cellulose samples prepared, for example, by acid hydrolysis. Based on spectrum appearance, the determined proportions of crystalline fibril interior, of slightly less ordered para-crystalline cellulose (PC), and accessible and inaccessible fibril surfaces (AS and IAS) are used to estimate the widths of fibrils and fibril aggregates, see Fig. 1a and b. (Larsson et al. 1997; Wickholm et al. 1998; Zhou et al. 2009; Malm et al. 2009).

The estimated total crystallinity [sum of I ($\alpha + \beta$) and PC] and cellulose fibril aggregate widths are reported Table 2. As can be seen in Table 2 the total crystallinity is in the same range (53–58 %). The fibril widths were estimated to 4.2–4.7 nm for all the pulps. Peak overlap of crystalline peaks and IAS peak make the calculations uncertain for the fibril widths and therefore differences between the pulps in fibril width are too small to be interesting for further discussion. Also the initial cellulose fibril aggregate widths were similar for the different pulps (17.5–17.8 nm, Table 2), and as mentioned above the three chemical pulps examined in this study were chosen for this property.

The most noticeable result from the CP/MAS ^{13}C-NMR analysis is the change in cellulose fibril aggregate width. Regarding the cellulose fibril aggregate width any overlap from the crystalline peaks does not interfere with calculations since these are based only

Table 1 Carbohydrate composition determined by neutral sugar analysis for the starting pulps and their polydispersity index (PDI) and weight average molar masses (M_w) determined by SEC, the low molecular mass represents the hemicelluloses and the high molecular mass the cellulose

	Glucose (wt%)	Xylose (wt%)	Mannose (wt%)	Arabinose (wt%)	Galactose (wt%)	Low M_w (10^3 g/mol)	High M_w (10^3 g/mol)	PDI
Kraft pulp	84.9	7.7	6.3	0.7	0.3	25.8	1,070	12.5
Sulfite pulps								
Dissolving grade	95.9	1.7	2.5	0.0	0.0	6.10	589	10.5
Paper grade	88.8	3.3	7.8	0.0	0.0	6.66	1,220	29.3

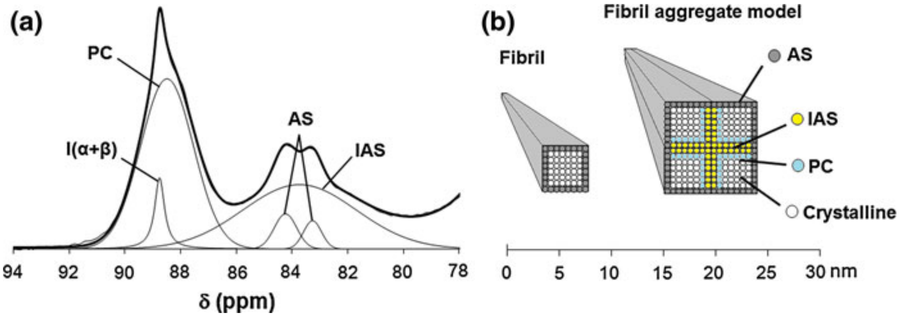

Fig. 1 **a** CP/MAS ^{13}C-NMR spectral fitting profiles of the C4 regions of a compression molded sulfite dissolving grade pulp (*PC* para-crystalline, *AS* accessible fibril surface, *IAS* inaccessible fibril surface). **b** Schematic representation of a fibril (width 4.4 nm) and a cellulose fibril aggregate (mean width 20 nm), in the calculation and in this figure assumed to have a square cross section. For authentic micrographs see ref. (Fink et al. 1995; Wickholm et al. 1998; Hult et al. 2001; Duchesne et al. 2001)

Table 2 Cellulose fibril aggregate widths (hydrolyzed samples except the dissolving grade) obtained by spectral fitting of the C4 region of the CP/MAS ^{13}C-NMR spectrum (reported with the standard error in parentheses) and the total crystallinity [sum of I ($\alpha + \beta$) and PC] of the starting and compression molded pulps

	Total crystallinity (%)		Cellulose fibril aggregate width (nm)	
	Starting pulp	Compression molded	Starting pulp	Compression molded
Kraft pulp	56 (1.0)	57 (1.0)	17.8 (0.70)	20.5 (1.11)
Sulfite pulps				
Dissolving grade	53 (0 5)	54 (0.5)	17.8 (0.34)	31.9 (1.25)
Paper grade	58 (0.8)	58 (0.8)	17.5 (0.69)	22.1 (0.92)

on the fibril surface peaks (AS and IAS). In a previous study it was found that the cellulose fibril aggregation increases with pressing temperature when compression molding dissolving pulps, reaching a maximum width at 170 °C (Nilsson et al. 2010). According to Table 2 cellulose fibril aggregation barely takes place upon compression molding in the kraft pulp, whereas somewhat larger cellulose fibril aggregates are formed in the sulfite dissolving grade pulp. In the sulfite paper grade pulp, cellulose fibril aggregation occurs although it is less compared with the dissolving grade. The results agree with earlier studies indicating that removal of hemicelluloses increase contact between cellulose fibril surfaces and hence increase the cellulose fibril aggregation (Hult et al. 2001; Duchesne et al. 2001; Chunilall et al. 2010).

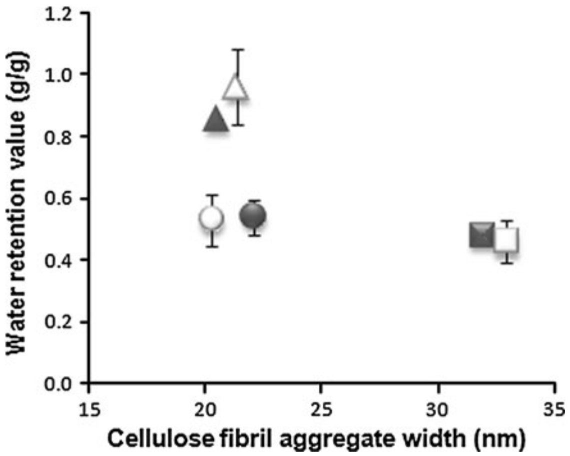

Fig. 2 Modified WRV versus cellulose fibril aggregate width determined by CP/MAS ^{13}C-NMR C4 spectral fitting for the compression molded sulfite dissolving grade pulp (*filled square*), sulfite paper grade pulp (*filled circle*) and paper grade kraft pulp (*filled triangle*) (*solid dots* represent beaten pulps and *clear dots* non-beaten pulps)

Water retention value (WRV) and hemicellulose structure/distribution

The importance of the differences in the hemicellulose structures between the sulfite and the kraft pulp is observed in the WRV of the molded pulps (Fig. 2). Although only a minor difference in the total hemicellulose content between the kraft and sulfite paper grade pulps, the compression molded sulfite paper grade pulp has a much lower WRV (0.5 g/g) than the kraft pulp (0.9 g/g). Neither the WRV nor the cellulose fibril aggregate widths of the molded pulps are affected by beating, hence any difference between the sulfite and kraft pulp in beating response cannot be related to the result. More likely, one of the explanations to this phenomenon could be chemical composition and structure of the hemicellulose. According to Table 1 the kraft pulp contains both arabinose and galactose as hemicellulose side groups (Jacobs and Dahlman 2001), whereas the sulfite pulp hemicelluloses do not contain discernable amounts of these constituents. Consequently, the more linear character of hemicelluloses and their lower molar masses in the sulfite paper grade pulp could perhaps make it possible for the hemicellulose to co-aggregate with cellulose fibril aggregates, resulting in slightly higher cellulose fibril aggregation and substantially lower WRV.

Another possible factor affecting the cellulose fibril aggregation is the distribution of the hemicelluloses on the fiber surfaces and in the fiber wall. Hemicelluloses present inside the fiber cell wall acts as spacers between cellulose fibril aggregates inhibiting further aggregation. Recently two types of xylan signals could be assigned in CP/MAS ^{13}C-NMR spectra of a birch kraft pulp; xylan inaccessible to hydrolysis by xylanase at 83.5 ppm and xylan accessible to hydrolysis by xylanase at 81.7 ppm (Teleman et al. 2001). A similar situation can be identified with two hemicelluloses signals; one at 81.9 ppm and another at 83.1–84.1 ppm also observed in galactoglucomannan containing kraft pulps (Wickholm et al. 1998; Hult et al. 2000). As a consequence we assign the signal at 83.5 ppm to enzyme inaccessible hemicelluloses, hereafter called inaccessible hemicelluloses (IH), present as co-aggregates with cellulose fibril aggregates inside the fiber wall (Teleman et al. 2001) and the signal at 81.0 ppm to hemicelluloses localized at fiber surfaces hereafter called accessible hemicelluloses (AH) (Fig. 3a, c). The relative contribution of xylan and glucomannan to the respective signal intensities cannot be determined by CP/MAS ^{13}C-NMR spectra due to signal overlap.

(a) Kraft, non-hydrolyzed (b) Kraft, hydrolyzed

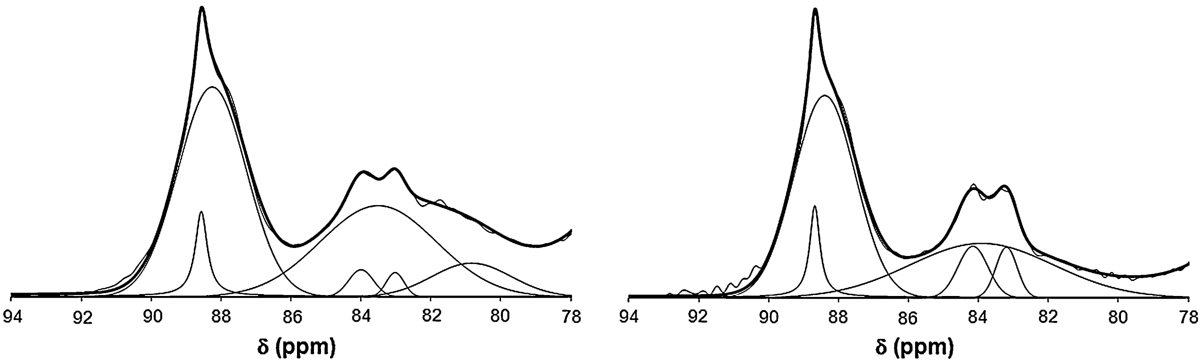

(c) Sulfite paper grade, non-hydrolyzed (d) Sulfite paper grade, hydrolyzed

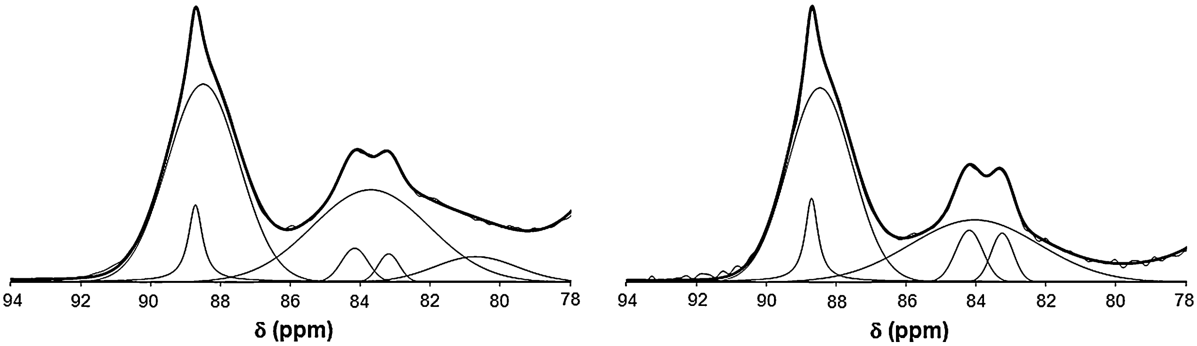

Fig. 3 CP/MAS ^{13}C-NMR spectral fitting profiles of the C4 regions of the following compression molded samples. **a** Kraft non-hydrolyzed, **b** kraft hydrolyzed, **c** sulfite paper grade non-hydrolyzed and **d** sulfite paper grade hydrolyzed

Table 3 Relative intensities of assigned peaks in the spectral fitting of the C4 region of the CP/MAS ^{13}C-NMR spectrum of non-hydrolyzed compression molded pulps (data with the SE in parentheses)

	Crystalline[a] (mol%)	IAS + IH[b] (mol%)	AS[c] (mol%)	AH[d] (mol%)	IH[e] (mol%)	Total hemi-cellulose content[f] (mol%)
Kraft pulp	53 (0.6)	35 (0.5)	3.7 (0.4)	8.7 (0.3)	9.5	18.2
Sulfite pulps						
Dissolving grade	54 (0.4)	39 (0.3)	7.0 (2.7)	nd	4.6	4.6
Paper grade	53 (0.5)	36 (0.4)	5.0 (0.4)	6.9 (0.2)	7.5	14.4

nd Not detected

The total hemicellulose contents according neutral sugar analysis calculations are also reported

[a] Crystalline = sum of I ($\alpha + \beta$) and PC

[b] IAS + IH = sum of inaccessible fibril surfaces (IAS) and IH at 83.5 ppm

[c] *AS* accessible fibril surface

[d] *AH* accessible hemicelluloses at 81 ppm

[e] *IH* inaccessible hemicelluloses at 83.5 ppm calculated as the difference between the total hemicellulose content and the accessible hemicelluloses at 81.0 ppm

[f] Total hemicellulose content in mol% based on neutral sugar analysis calculations according to Jansson (1970)

In Table 3 the relative intensities of assigned peaks of the non-hydrolyzed pulp samples are shown (Fig. 3a–d). By subtracting the intensities of the hemicelluloses signal at 81.0 ppm from the total hemicellulose content in mol% based on neutral sugar analysis calculations according to Jansson (1970) it is possible to estimate the IH contribution to the 83.5 ppm signal. Consequently, by combining NMR analysis with neutral sugar analysis it is possible to approximate the distribution of the hemicellulose in the fiber cell wall.

From the given results it is difficult to interpret whether it is the total hemicellulose content or the distribution of the hemicelluloses in the fiber cell wall that determines the cellulose fibril aggregation (Fig. 4). As mentioned above, one interpretation of the results related to the low WRV of the compression molded sulfite pulps is that the actual fibril aggregate are larger in these samples due to the proposed ability of the more linear and smaller hemicelluloses to co-aggregate with cellulose fibril aggregates.

Mechanical properties

Young's modulus is a property of particular interest since its relationship to composite structure is more direct than measured strength which depends on interacting failure mechanisms on the fiber network level, as well as the size and orientation of the largest defect in the test volume. In the previous study by Nilsson et al. (2010) is was suggested that the combination of pressure and temperature during

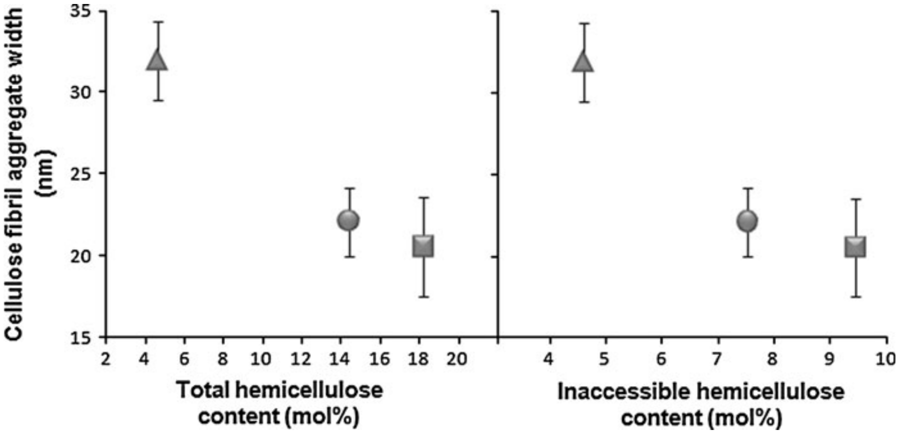

Fig. 4 Cellulose fibril aggregate width versus total and IH content determined by calculations according to Jansson (1970) and CP/MAS ^{13}C-NMR C4 spectral fitting of the compression molded sulfite dissolving grade pulp (*filled square*), sulfite paper grade pulp (*filled circle*) and paper grade kraft pulp (*filled triangle*)

Table 4 Mechanical properties and densities of the compression molded pulps (data with SD in parentheses)

	Young's modulus (GPa)	Ultimate tensile strength (MPa)	Strain to failure (%)	Density (g/cm^3)
Kraft pulp	6.3 (3.0)	109 (7.2)	6.3 (1.4)	1.28 (0.02)
Sulfite pulps				
Dissolving grade	11.5 (2.4)	75.1 (4.5)	2.0 (0.1)	1.32 (0.04)
Paper grade	12.0 (2.1)	74.0 (3.4)	2.4 (0.3)	1.27 (0.01)

compression molding leads to improved interfiber fusion bonding at high temperatures (150–180 °C) under pressure resulting in a higher modulus of the biocomposite. In this study the main issue is the differences between different chemical pulps in hemicellulose content, structure and distribution in combination with the effect of compression molding. Both the sulfite pulps exhibit Young's modulus around 11–12 GPa, whereas the kraft pulp only possess half of that level around 6 GPa (Table 4). Hence, the difference in total hemicellulose content between the sulfite dissolving and paper grade pulp (4.6 and 14.4 mol% respectively) cannot be correlated to the Young's modulus. As seen in Table 4, compression

(a) Kraft paper grade pulp

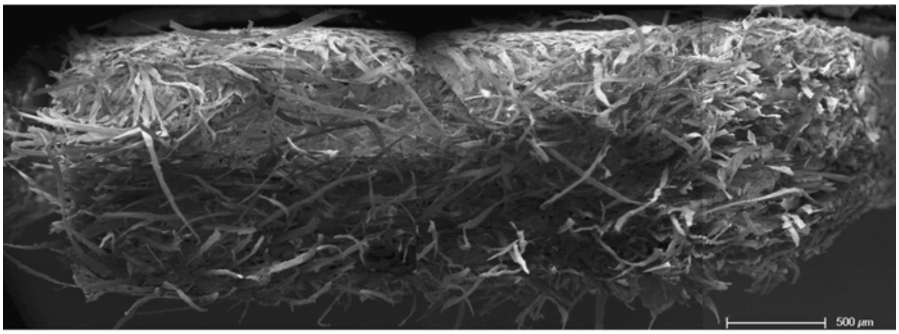

(b) Sulfite dissolving grade pulp

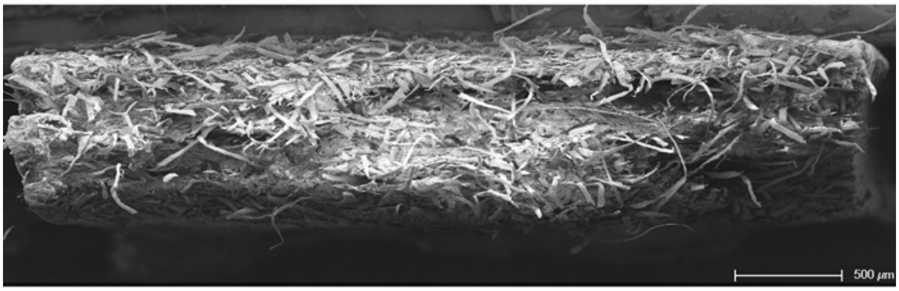

(c) Sulfite paper grade pulp

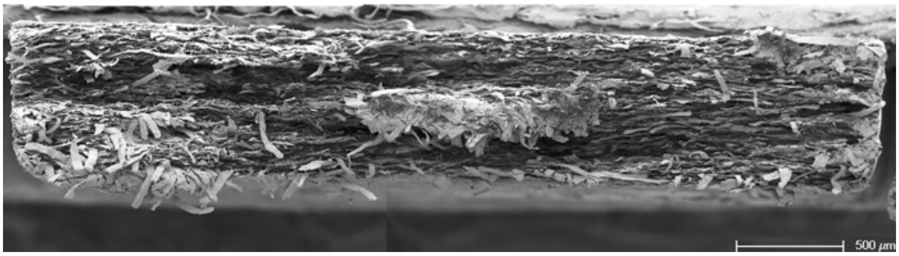

Fig. 5 FE–SEM cross-section micrographs at ×50 of magnification of tensile fracture surfaces of compression molded kraft pulp (**a**), sulfite dissolving grade pulp (**b**) and sulfite paper grade pulp (**c**)

molding results in similar densities for all the pulps so neither this is the reason.

An important difference between sulfite and kraft pulp regarding the mechanical properties is the well known fact that sulfite pulps are easier to beat (Ahlgren et al. 1975; Petterson and Rydholm 1960; Giertz 1953). The more fibrillated surface of the sulfite pulp fibers most likely improves interfibre bonds resulting in a high Young's modulus. The weaker interfibre bonds of the kraft pulp explain the higher ultimate strength due to higher strain to failure (6%) as compared to the high modulus sulfite pulp based ones (2%).

The difference between the sulfite pulps and kraft pulp in terms of fiber-pull-out during fracture is shown in the SEM micrographs in Fig. 5. The fiber pull-outs in the fracture surface of the compression molded kraft pulp are extensive compared to the compression molded sulfite pulps with a more brittle fracture.

Conclusion

Compression molding of chemical wood pulps yields biocomposites with material properties that can be correlated to the pulping method. Biocomposites based on acid sulfite dissolving grade pulp or sulfite paper grade pulp exhibit twice as high Young's modulus as the composite based on paper grade kraft pulp, 11–12 and 6 GPa, respectively. Also the WRV is similarly low for the two molded sulfite pulps (0.5 g/g) as compared to the molded kraft pulp (0.9 g/g). Since the total hemicellulose content is on a comparable high level for both the paper grade sulfite (14.4 wt%) and kraft pulp (18.2 wt%), in contrast to the sulfite dissolving grade pulp (4.6 wt%), any difference in total hemicellulose content cannot be related to the material properties. The beating response of the kraft and sulfite pulp differs and this could explain the different mechanical properties of the molded pulps since the sulfite pulps are more sensitive to beating. On the other hand, the WRV is not affected by beating. A tentative explanation is instead correlated to the suggested ability of the more linear and smaller sulfite hemicelluloses, unlike the kraft hemicelluloses, to form co-aggregates with the cellulose fibril aggregates. Cellulose fibril aggregation is hence connected to the WRV but from this study it not possible to determine if it is the total hemicellulose content or the hemicellulose distribution inside the fiber cell wall that controls the cellulose fibril aggregation. In conclusion, it should be emphasized that it is possible to attain high-stiffness biocomposites by compression molding of commercial chemical pulps and by controlling the hemicellulose structure and/or distribution it could be possible to direct the water sensitiveness of new wood pulp based materials.

Acknowledgments This work was supported by Swedish Centre for Biomimetic Fibre Engineering (Biomime) and Research Institutes of Sweden (Rise). Domsjö Fabriker AB is acknowledged for gifts of sulfite pulps.

References

Ahlgren P, Olsson PA, Vikström B (1975) Comparision between the properties of high yield conventional kraft pulp and those of polysulfide and hydrogen sulfide yield pulps. Sven Papperstidn 78:75–102

Berthold F, Gustafsson K, Berggren R, Sjöholm E, Lindström M (2004) Dissolution of softwood kraft pulps by direct derivatization in lithium chloride/*N*,*N*-dimethylacetamide. J Appl Polym Sci 94:424–431

Chunilall V, Bush T, Larsson PT, Iversen T, Kindness A (2010) CP/MAS ^{13}C-NMR study of cellulose fibril aggregation in eucalyptus dissolving pulps during drying and the correlation between aggregate dimensions and chemical reactivity. Holzforschung 64:693–698

Duchesne I, Hult EL, Molin U, Daniel G, Iversen T, Lennholm H (2001) The influence of hemicellulose on fibril aggregation of kraft pulp fibres as revealed by FE-SEM and CP/MAS ^{13}C-NMR. Cellulose 8:103–111

Fengel D, Wegner G (1984) In wood: chemistry, ultrastructure, reactions. Walter de Gryter, Berlin, p 66

Fink HP, Hofmann D, Philipp B (1995) Some aspects of lateral chain order in cellulosics from X-ray scattering. Cellulose 2:51–70

Frey-Wyssling A (1954) The fine structure of cellulose microfibrils. Science 119:80–82

Giertz HW (1953) En jämförelse mellan sulfit- och sulfatmassa. Sven Papperstidn 56:893–899

Hult EL, Larsson PT, Iversen T (2000) A comparative CP/MAS ^{13}C-NMR study of cellulose structure in spruce wood and kraft pulp. Cellulose 7:35–55

Hult EL, Larsson PT, Iversen T (2001) Cellulose fibril aggregation—an inherent property of kraft pulps. Polymer 42:3309–3314

Iwamoto S, Kai W, Isogai A, Iwata T (2009) Elastic modulus of single cellulose microfibrils from tunicate measured by atomic force microscopy. Biomacromolecules 10: 2571–2576

Jacobs A, Dahlman O (2001) Characterization of the molar masses of hemicelluloses from wood and pulps employing size exclusion chromatography and matrix-assisted laser desorption ionization time-of-flight mass spectroscopy. Biomacromolecules 2:894–905

Jansson J (1970) Calculation of the polysaccharide composition of wood and pulp. Pap Puu 5:323–329

Larsson PT, Wickholm K, Iversen T (1997) A CP/MAS ^{13}C-NMR investigation of molecular ordering in celluloses. Carbohydr Res 302:19–25

Malm E, Bulone V, Wickholm K, Larsson PT, Iversen T (2009) The surface structure of well-ordered native cellulose fibrils in contact with water. Carbohydr Res 11:97–100

Nilsson H, Galland S, Larsson PT, Gamstedt EK, Nishino T, Berglund LA, Iversen T (2010) A non-solvent approach for high-stiffness all-cellulose biocomposites based on pure wood cellulose. Compos Sci Technol 70:1704–1712

Nishino T, Matsuda I, Hirao K (1995) Elastic-modulus of the crystalline regions of cellulose polymorphs. J Polym Sci B Polym Phys 33:1647–1651

Petterson SE, Rydholm SA (1960) Hemicelluloses and paper properties of birch pulps. Sven Papperstidn 63:4–17

Sakurada I, Nukushina Y, Ito T (1962) Experimental determination of the elastic modulus of crystalline regions in oriented polymers. J Polym Sci 57:651–660

Teleman A, Larsson PT, Iversen T (2001) On the accessibility and structure of xylan in birch kraft pulp. Cellulose 8:209–215

Wickholm K, Larsson PT, Iversen T (1998) Assignment of non-crystalline forms in cellulose I by CP/MAS ^{13}C-NMR spectroscopy. Carbohydr Res 312:123–129

Zhou Q, Malm B, Nilsson H, Larsson PT, Iversen T, Berglund LA, Bulone V (2009) Nanostructured biobiocomposites based on bacterial cellulosic nanofibers compartmentalized by a soft hydroxyethylcellulose matrix coating. Soft Matter 5:1–8